20633

Authorized Reprint 1989 from Special Technical Publication 995 1989

Marion F. Mecklenburg,[1] *James A. Joyce,*[2] *and Pedro Albrecht*[3]

Separation of Energies in Elastic-Plastic Fracture

REFERENCE: Mecklenburg, M. F., Joyce, J. A., and Albrecht, P., **"Separation of Energies in Elastic-Plastic Fracture,"** *Nonlinear Fracture Mechanics: Volume II—Elastic-Plastic Fracture, ASTM STP 995,* J. D. Landes, A. Saxena, and J. G. Merkle, Eds., American Society for Testing and Materials, Philadelphia, 1989, pp. 594–612.

ABSTRACT: The area under load versus the load-line displacement record represents the sum of the stored potential energy, the released elastic energy, and the dissipated plastic energy necessary to grow a crack through a test specimen. When partitioned as presented in this paper, these energy components can be evaluated in terms of current elastic-plastic fracture parameters. The authors show that the elastic energy release rate, G, as calculated by measuring the appropriate component from the test record, is identical to G calculated from K_q. The plastic energy dissipated, as measured directly from the load-displacement record, represents a much higher value than would be indicated by current J-type calculations.

In all cases examined, it is further shown that energy released or dissipated is strongly dependent on the size of the test specimen and the size of the initial crack length. Further, while the rolling orientation and prestraining of the steels investigated affect the plastic energy dissipation rate, there seems to be little effect on the elastic energy release rate.

KEY WORDS: elastic-plastic fracture, stable crack growth, specimen size effects, energy separation, fracture mechanics, nonlinear fracture mechanics

The objectives of this study are (1) to separate the total energy in the specimen, as represented by the load-displacement record, into its elastic and plastic components; (2) to relate the changes of these energy components, with respect to crack size, to the elastic and plastic fracture characterization parameters computed by the stress singularity approach; and (3) to apply the methodology to the analysis of specimens with different crack lengths, sizes, orientation, and prestrain.

Analysis

The background data assumed for this analysis comprise the standard unloading compliance load versus load-line displacement record, as shown in Fig. 1. This curve is the record of the total energy a fracture specimen stores, releases, or dissipates during an increment of displacement between consecutive unloadings. The work done by the external load can be related to the internal energy by

$$dW = dU_s + dU_e + dU_p \tag{1}$$

[1] Research engineer, Smithsonian Institution, Washington, DC 20560.
[2] Professor, Department of Mechanical Engineering, U. S. Naval Academy, Annapolis, MD 21402.
[3] Professor, Department of Civil Engineering, University of Maryland, College Park, MD 20742.

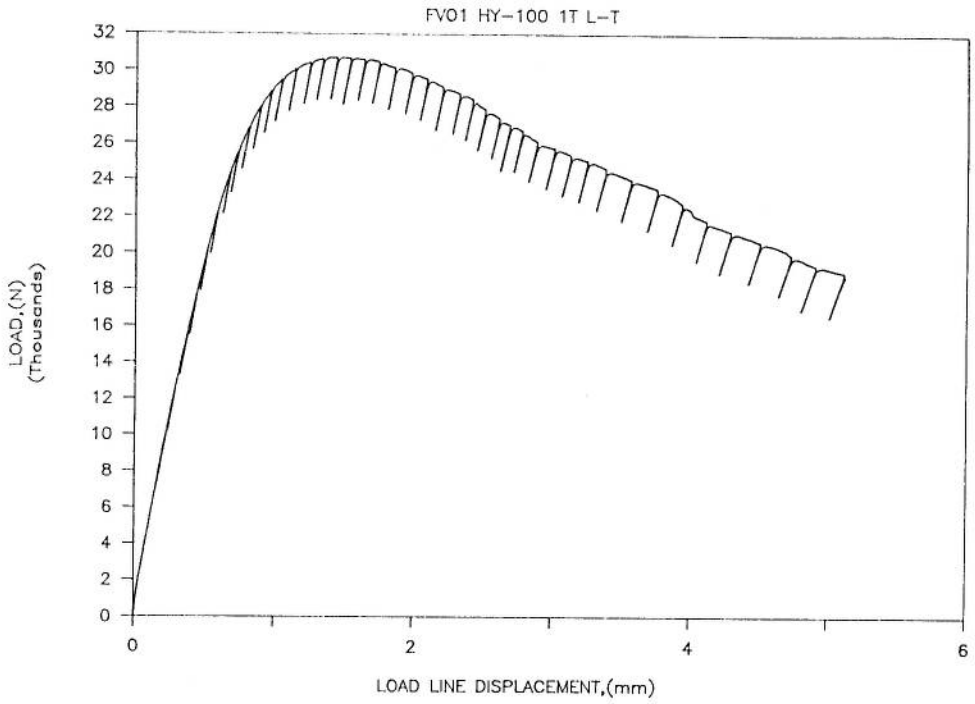

FIG. 1—*Standard unloading compliance, showing the load versus load-line displacement record for a compact tension specimen.*

where

W = work done by external load,
U_s = stored elastic strain (potential) energy,
U_e = elastic energy released during crack extension, and
U_p = plastic energy dissipated during crack extension.

These energies are illustrated for an elastic material, for an elastic-plastic material, and for the typical unload compliance test in Fig. 2.

In reviewing Fig. 2*c*, the total energy resisting a crack growth increment, Δa, is the sum of the dissipated plastic energy represented by the area OAA′O′ and the released elastic energy, area O′A′B. This can be expressed mathematically by

$$J = G + I = \frac{1}{B_n}\frac{dU_e}{da} + \frac{1}{B_n}\frac{dU_p}{da} \tag{2}$$

where

J = the total rate of energy input to the specimen,
G = the elastic energy release rate,
I = the plastic energy dissipation rate, and
B_n = the net specimen width between side grooves.

The stored elastic energy, area O′BD, is not included in Eq 2.

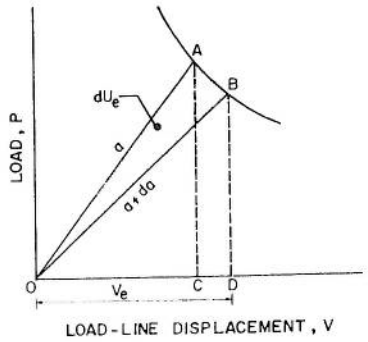

FIG. 2—*Energy components defined for typical load-displacement records:* (a) *elastic components.*

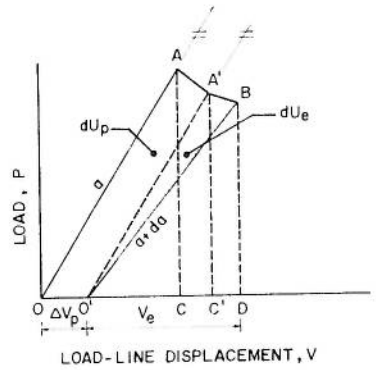

FIG. 2—*Continued:* (b) *elastic-plastic components.*

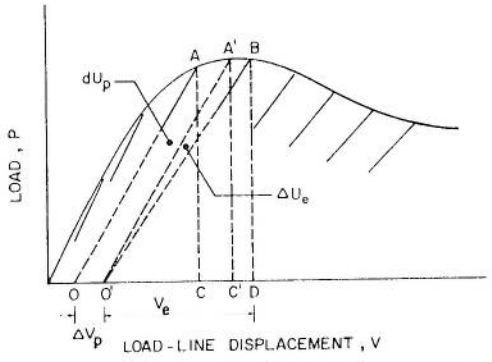

FIG. 2—*Continued:* (c) *unloading compliance component.*

Since there is an extensive archive of test data stored, either in the form of computer magnetic media or graphic records which can be digitized, the energy separation technique can be used to reexamine a wide variety of materials, specimen types, and pretest processes, such as prestraining. Much of this material is available from the U.S. Naval Academy, and the David Taylor Naval Ship Research and Development Center, both in Annapolis, Maryland, and from Materials Engineering Associates, Lanham, Maryland.

To illustrate the results of energy separation, a 1T compact specimen, with the load versus load-line displacement record shown in Fig. 1, is presented in Fig. 3. For this high-toughness steel, HY-100, the plastic component dissipated is much larger than either the released elastic energy or the stored elastic energy. On an enlarged scale, as shown in Fig. 4, it can be seen that the elastic energy released per unit of crack extension, dU_e/da, remains nearly constant over the extent of ductile crack extension examined, in this case, 20% of the initial net ligament.

For a strictly elastic condition

$$G = \frac{K^2(1 - \nu^2)}{E} \tag{3}$$

where K is the elastic stress-intensity factor establishing the intensity of the stress field near the crack tip, and G is the elastic release rate.

Taking here the quantity K_q, where K_q is evaluated from the equation in the ASTM Test

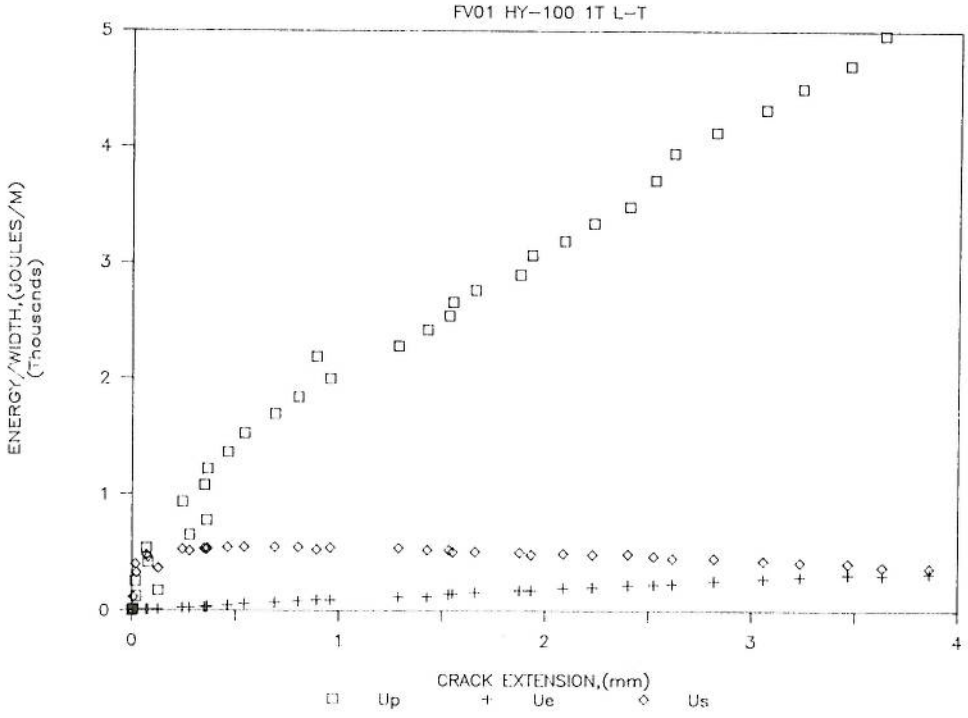

FIG. 3—*Energies dissipated, released, and retained versus crack extension.*

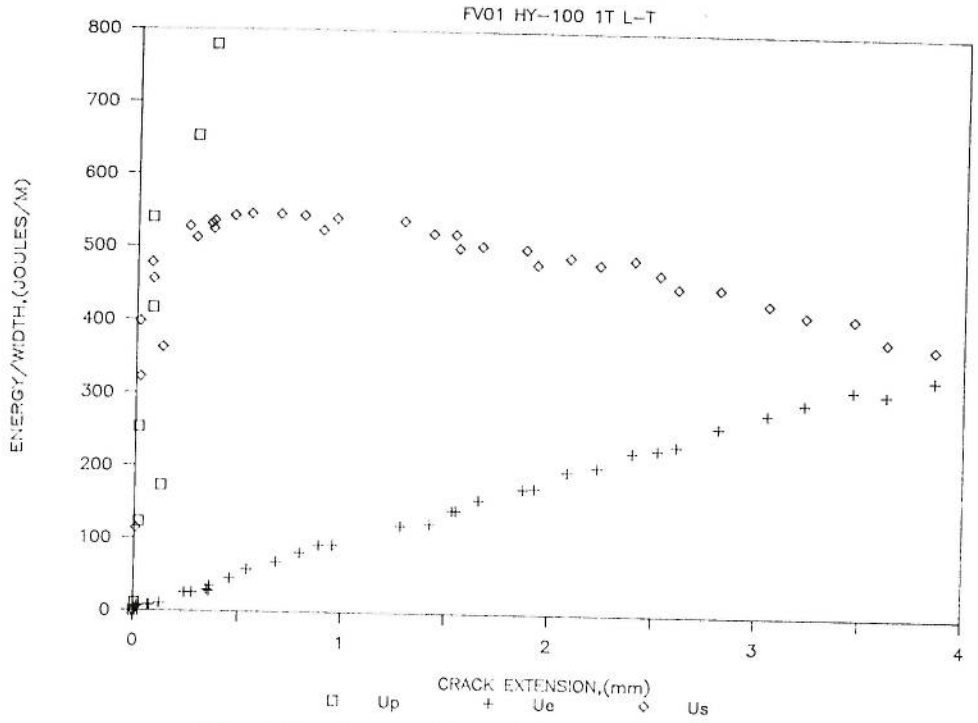

FIG. 4—*Energies released or retained versus crack extension.*

for Plane-Strain Fracture Toughness of Metallic Materials (E 399-83)

$$K_q = \frac{P}{B_n W^{1/2}} \cdot f\left(\frac{a}{W}\right) \tag{4}$$

where

$$f\left(\frac{a}{W}\right) = \frac{\left(2 + \frac{a}{W}\right)}{\left(1 - \frac{a}{W}\right)^{3/2}} \times \left[0.886 + 4.64\left(\frac{a}{W}\right) - 13.32\left(\frac{a}{W}\right)^2 + 14.72\left(\frac{a}{W}\right)^3 - 5.6\left(\frac{a}{W}\right)^4\right]$$

and P is the load value for each unloading taken just at the start of unloading, one can relate U_e to K_q in the following manner

$$\frac{U_e}{B_n} = \int G_q da = \int \frac{K_q^2(1 - \nu^2)}{E} da \tag{5}$$

Using a simple numerical summation procedure, one obtains the results plotted in Fig. 5.

in which U_e from the method of Eq 5 is compared with the direct results obtained from the energy separation method of Fig. 2*c*. The fact that the comparison shown is so good (and can be obtained in a similar fashion on a range of materials and specimen sizes) is rather remarkable. The direct evaluation method makes no assumptions of material properties, and yet it obtains an elastic energy that corresponds to the result of applying elastic equations to a load displacement history which is far from elastic. The slope of the curve in Fig. 5 is the elastic energy release rate, G_q, corresponding to the elastic component of fracture toughness for that specimen, that material, and, as it will be shown, that a/W value.

Figure 6 shows the load versus the elastic component of the load-line displacement. This plot is typical of an elastic material and matches the Type III load-displacement record of ASTM Test E 399-83. It further confirms that G_q is the elastic energy release rate. The shaded area shown is the change in the elastic energy released, dU_e, between two consecutive unloadings.

The final step involves the calculation of the plastic energy dissipation rate, I, of Eq 2. This quantity, as well as the elastic energy release rate, G_q, and the sum of the two, J, are plotted versus the crack extension in Fig. 7. In this diagram, G_q rises rapidly to a nearly constant (though small) value, while I jumps to a high value and then falls, approaching a seemingly constant plateau.

The plastic energy dissipated and illustrated above includes all plastic energy related to the test specimen and not just plastic energy associated with the crack tip (fracture process zone). Since many of the tough steel specimens form full plastic hinges and reach limit loads during the test, much of the plastic energy dissipated is on the compression side of the neutral axis.

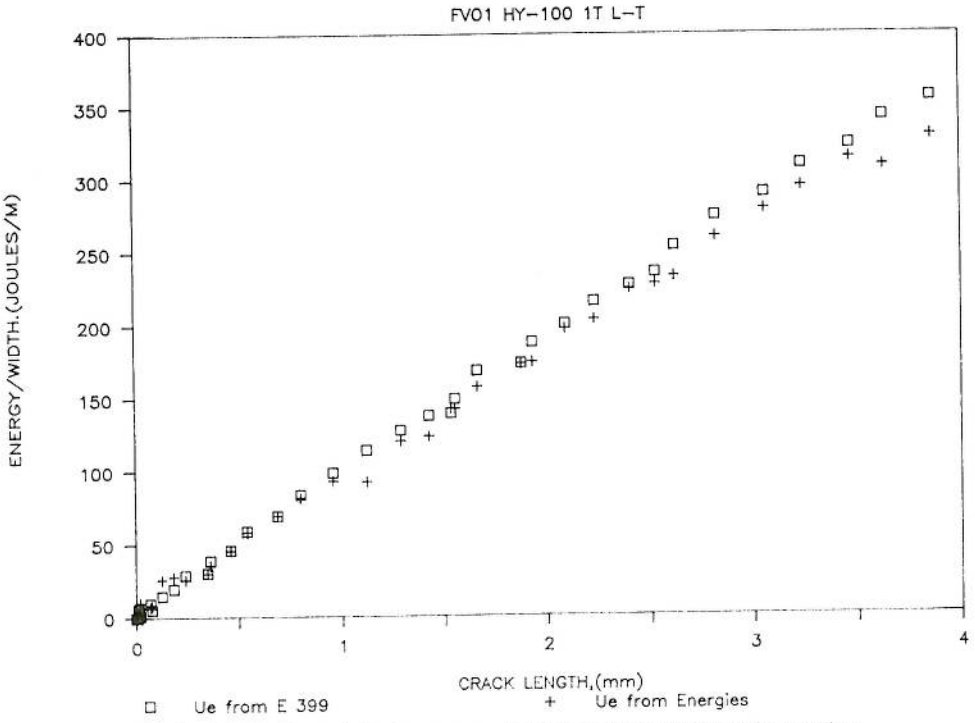

FIG. 5—*Comparison of elastic energy released as a function of crack extension.*

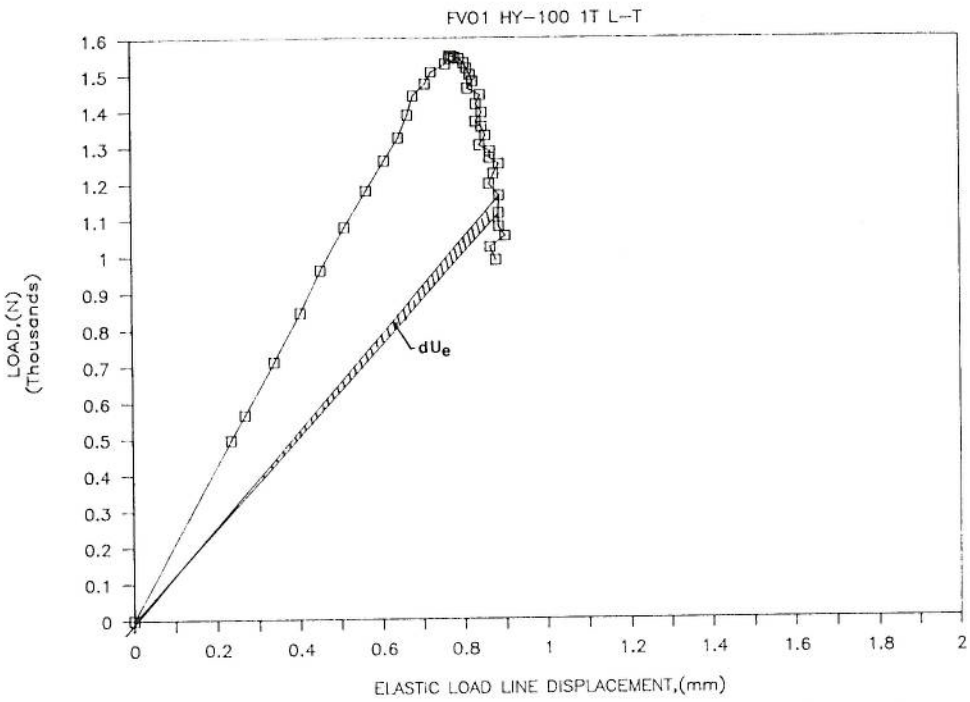

FIG. 6—*Load versus the elastic component of the load-line displacement. The shaded wedge represents the elastic energy released during an increment of crack extension.*

Since considerable plastic energy dissipated in the specimen is not related to the crack tip but to plastic deformation of the remaining ligament, one might expect to detect an influence of the specimen size and geometry. The remaining part of this paper will examine this topic.

Description of the Experiment

The method of energy separation can be applied to any set of unloading compliance data, and in the course of this work, it has been applied to many different materials and specimen geometries using the data base of specimens available at various sources. The results presented here are representative of what has been observed in the process. Since it is an empirical approach, we include in Table 1, for completeness, the standard material property data on the materials used. All specimens reported here are compact tension (CT) specimens made in accordance with the ASTM Test for J_{Ic}, a Measure of Fracture Toughness (E 813-81). Other geometries have been analyzed, and it appears that the results presented here are consistent with those obtained from simple test geometries. Since the preponderance of available data are CT data, these specimens have been used exclusively here. All specimens have 20% side grooves.

The energy separation method is applied in the following sections to four cases in which the specimens differ in (1) crack size, (2) scale (2T to 10T), (3) orientation, and (4) initial prestrain.

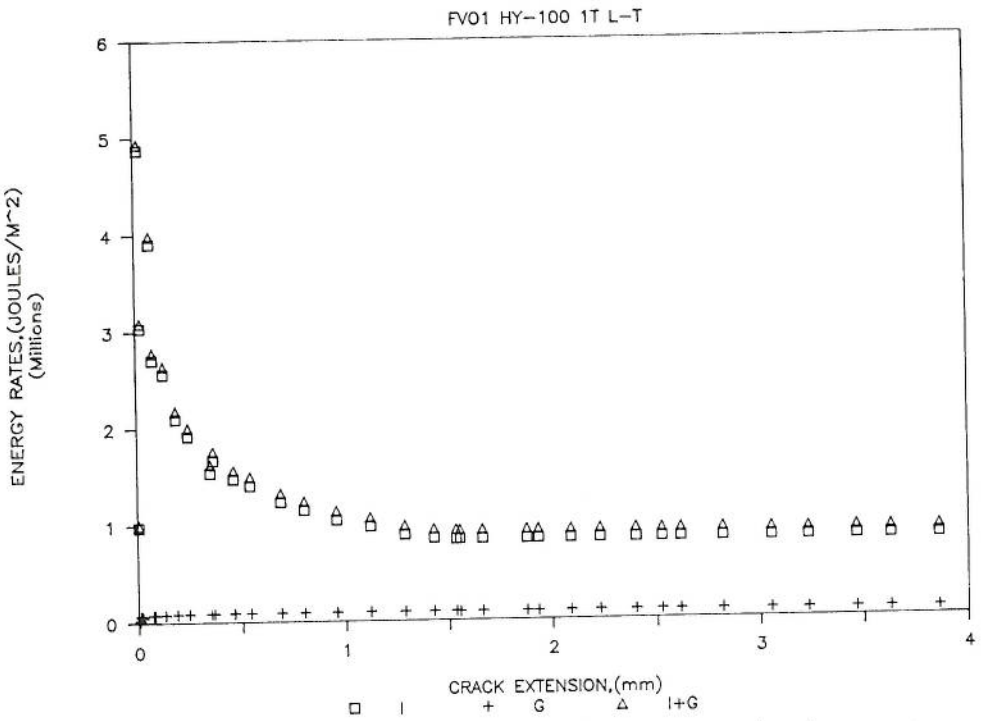

FIG. 7—*Elastic energy release rate, plastic energy dissipation rate, and total energy rate versus crack extension.*

Crack Size Dependence

The energy separation technique was used here to reanalyze a set of unloading compliance data previously reported [*1*] which contained compact specimens for the A533B steel whose tensile properties are shown in Table 1. These specimens were 1T compact specimens with 20% side grooves and fatigue precrack a/W values of 0.51, 0.62, 0.72, and 0.81. Application of the energy separation method to these specimens produces the results shown in Fig. 8. This figure shows the elastic energy released versus the crack extension and, while the slope is fairly constant over the crack extension range of each test, the slopes (G_q) differ greatly

TABLE 1—*Tensile properties of steels.*[a]

Series	Type of Steel	Specimen Diameter, in.	Displacement Rate, in./min	Tensile Strength, ksi	Yield Strength, 0.2% Offset, ksi	Elongation, %	Reduction of Area, %	Direction
FVO	HY-100	0.50	0.01	122	110	22	63	long
A533B	A533B	0.252	0.01	94	70	19	...	long
EPRI	A508 2A	...	...	80	55	30	63	...

[a] Metric conversion factors:
1 in. = 25.4 mm.
1 ksi = 6.8948 MPa.

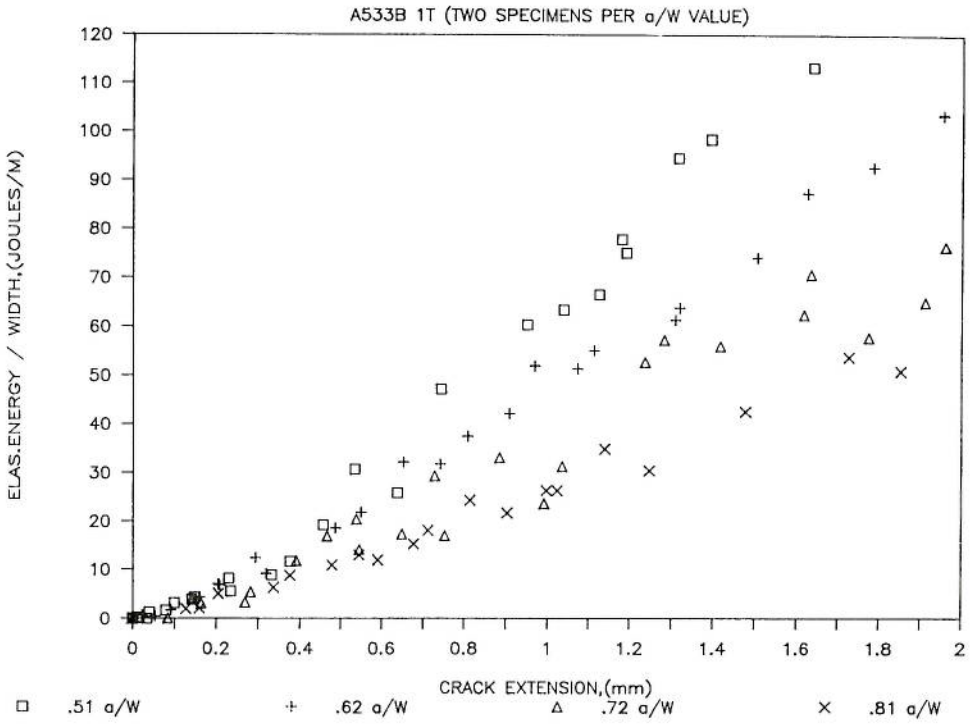

FIG. 8—*Elastic energy released for different initial crack length ratios versus crack extension.*

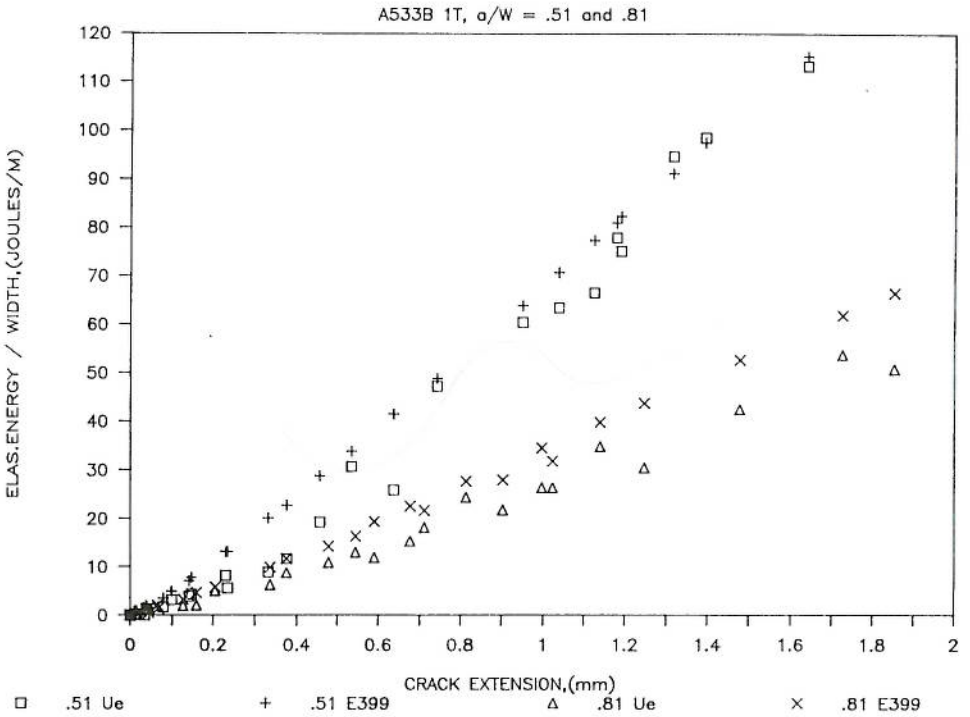

FIG. 9—*Elastic energy released, as calculated from ASTM Test E 399-83, and energy separation versus crack extension.*

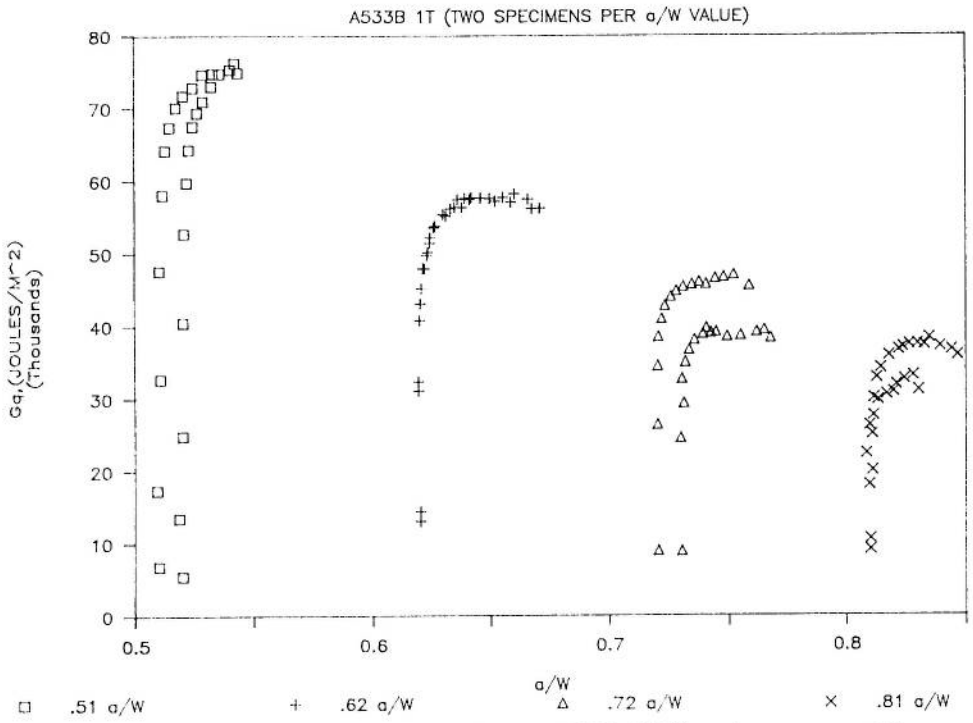

FIG. 10—*Elastic energy release rates for different A533B 1T CT specimens versus* a/W.

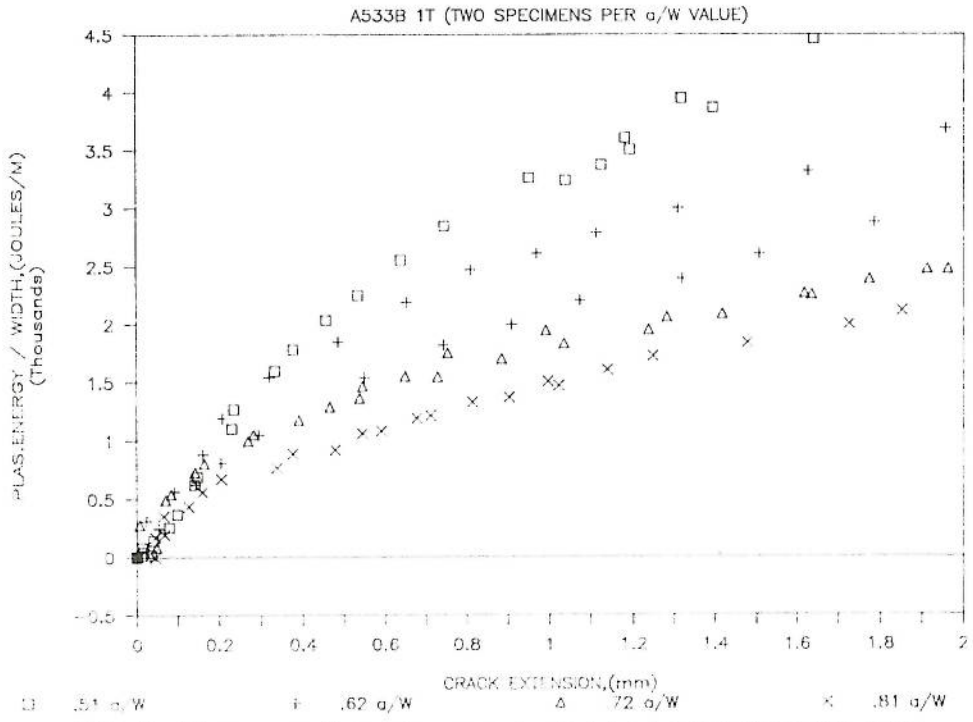

FIG. 11—*Plastic energy dissipated versus crack extension for different initial crack length ratios.*

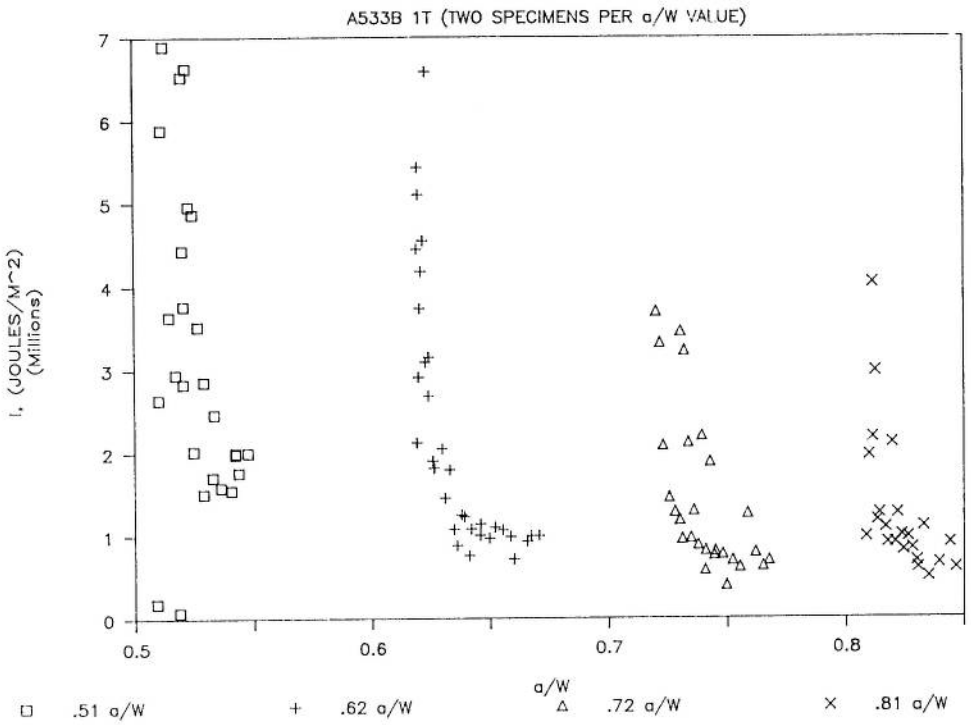

FIG. 12—*Plastic energy dissipation rates for different A533B 1T CT specimens versus* a/W.

in the different initial crack lengths. For each crack length ratio the elastic energy release measured directly from the load displacement record corresponds to that obtained from K_q using Eq 5. In other words $G = G_q$. The two extreme cases with $a/W = 0.51$ and 0.81 are shown in Fig. 9. The value G can then be defined as either the derivative of the curves in Fig. 8 or as it is defined in Eq 3. The values of G_q shown as a function of a/W in Fig. 10 vary strongly with the a/W ratio. The plastic energy dissipation U_p/B_n is also strongly dependent on the initial crack length, as shown in Fig. 11. As in the case of the elastic energy release rate, the value I, as defined in Eq 2, is the derivative of the curves in Fig. 11, and as shown in Fig. 12, these are also stongly dependent on the initial a/W ratios. However, crack size dependence is nearly eliminated for both G and I when divided by b, the remaining ligament length, as in the standard J-integral type relationship.

Specimen Size Dependence

Energy separation techniques were also applied to a data set of compact specimens run at Westinghouse Research [2] involving A508 steel specimens from ½T to 10T in size. The material property data are presented for this material in Table 1. In this study we examine only 10T, 4T, and 2T specimens. The elastic energy released as a function of crack extension is plotted in Fig. 13, and the plastic energy dissipated as a function of crack extension is shown on Fig. 14. As before, the energy components are very size dependent. What is of interest here is that the elastic energy released, as calculated from K_q, still corresponds to the energy released as directly computed. This is shown in Figs. 15, 16, and 17.

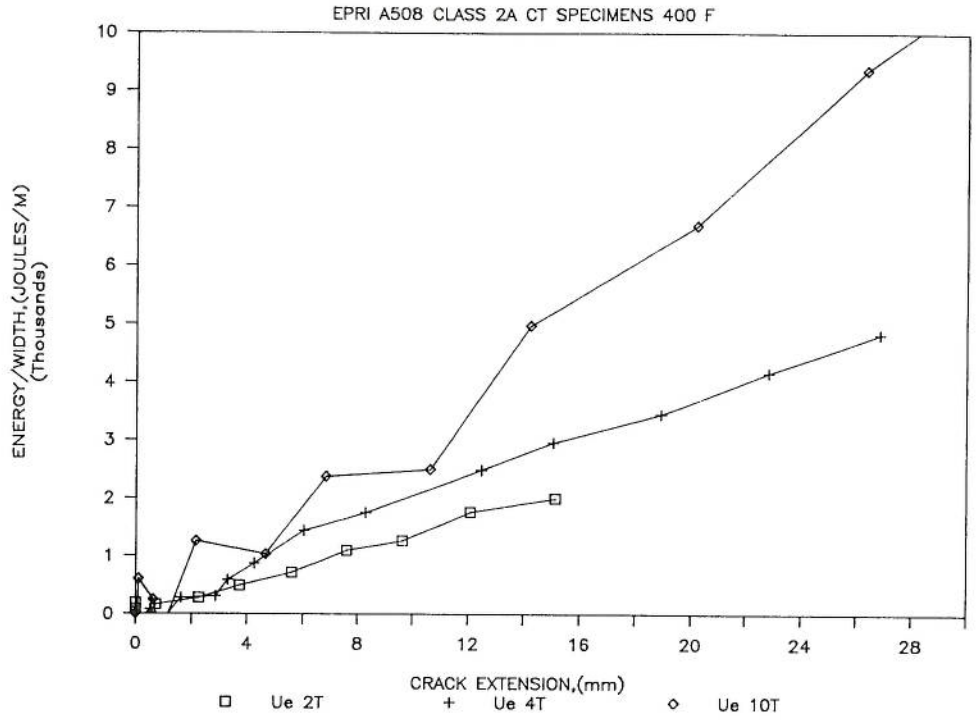

FIG. 13—*Released elastic energy versus crack extension for specimens of different size.*

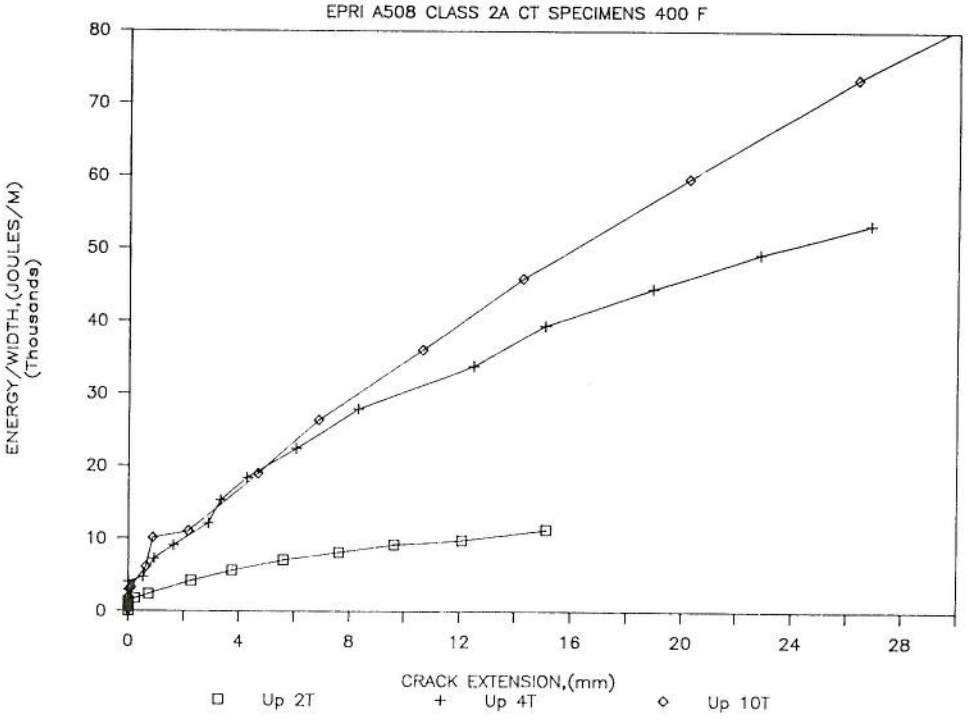

FIG. 14—*Dissipated plastic energy versus crack extension for specimens of different size.*

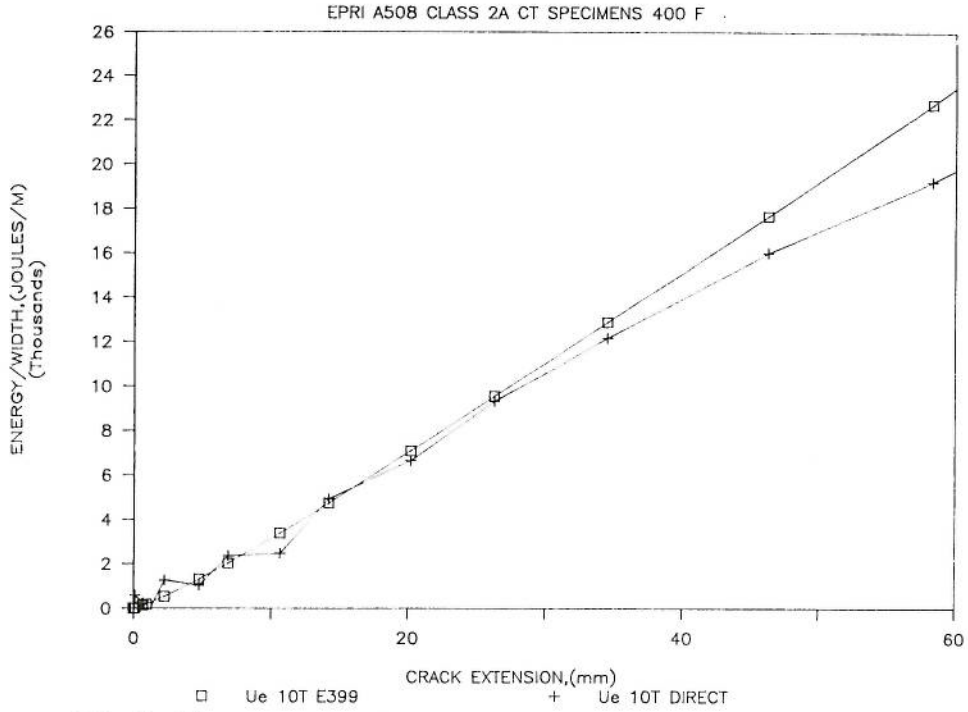

FIG. 15—*Elastic energy released versus crack extension from both the direct method and ASTM Test E 399-83.*

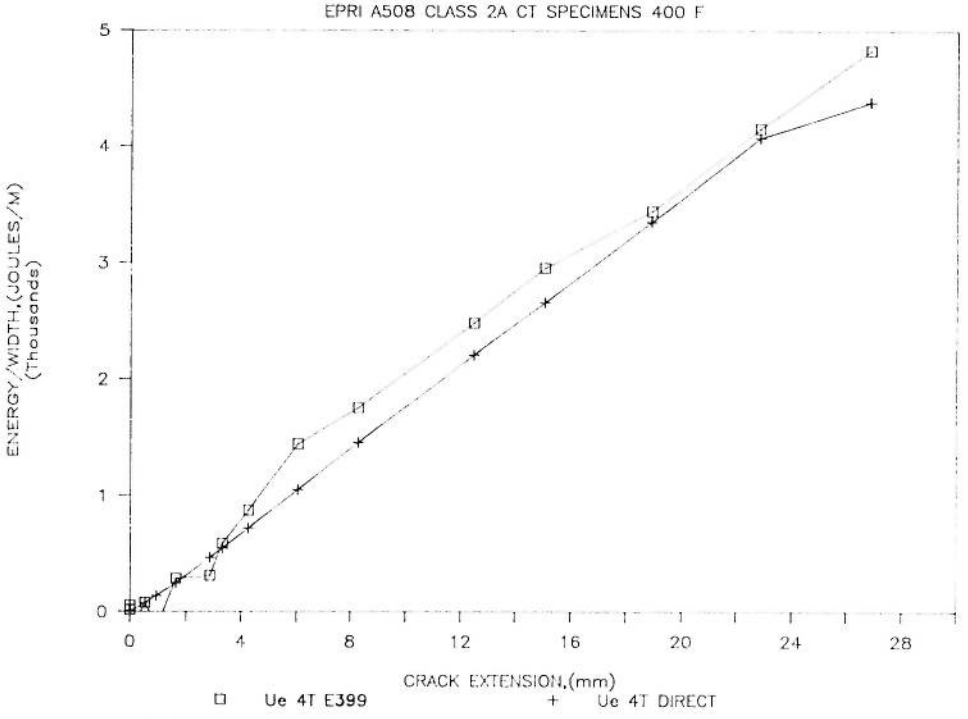

FIG. 16—*Elastic energy released versus crack extension from both the direct method and ASTM Test E 399-83.*

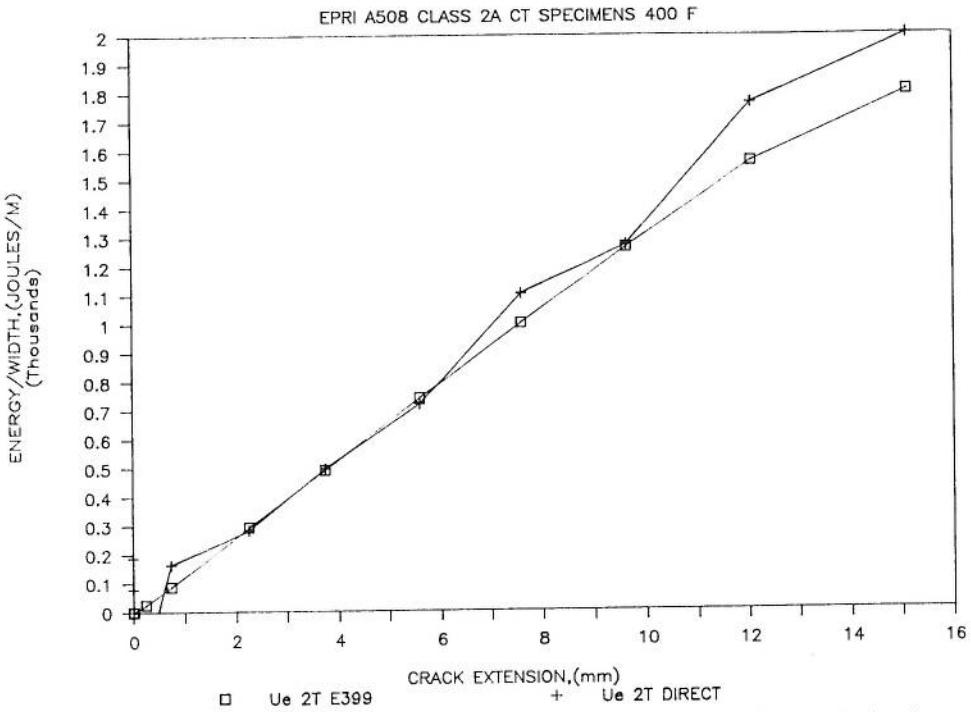

FIG. 17—*Elastic energy released versus crack extension from both the direct method and ASTM Test E 399-83.*

Specimen Orientation Dependence

Taking two 1T compacts of HY-100 [3] steel plate material with orientations of L-T and T-L, respectively, gives the energy plots shown in Figs. 18 and 19. Clearly the material orientation dramatically affects the plastic energy component, while the elastic energy release rate appears to be nearly the same for the two test orientations.

Uniform Specimen Prestrain Effects

Also included in the HY-100 data from Ref 3 are unloading compliance data for 1T compact specimens made from plate on which 0, 3, and 5% uniform uniaxial plastic prestrain had been applied. Figures 20 and 21 show that, while the plastic energy dissipated is reduced with increasing prestrain, the elastic energy release rate is not affected.

Observations on the Plastic Energy Dissipation Rate

The plastic energy dissipation rate, J, as defined by Eq 2, can be evaluated by taking the slope of the plastic energy plots presented above; that is, by evaluating

$$J = \frac{1}{B_n} \frac{dU_p}{da}$$

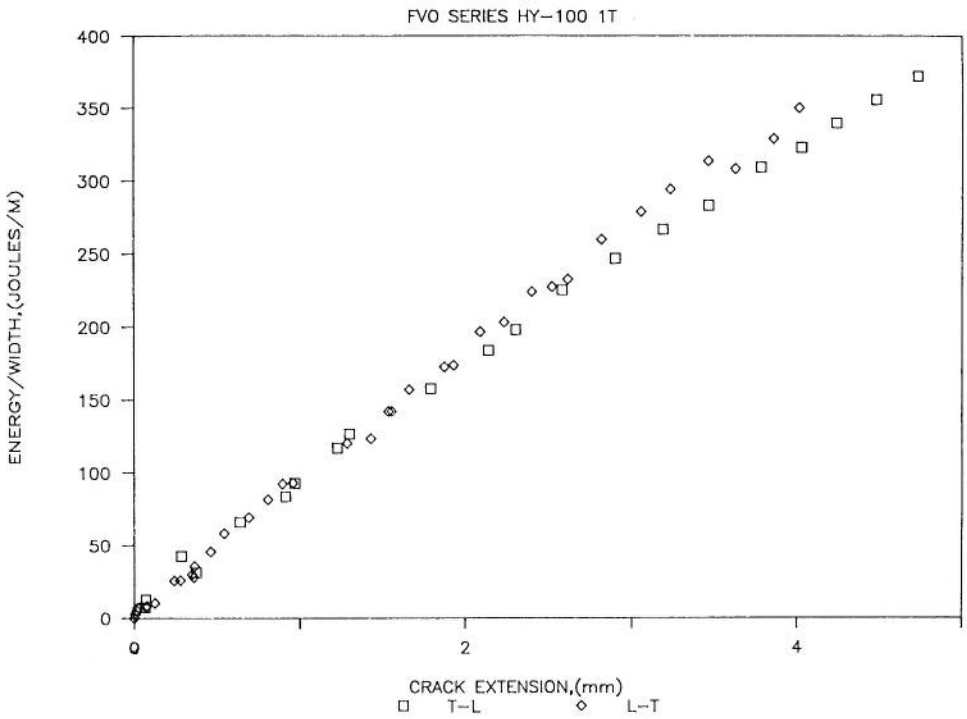

FIG. 18—*Effect of specimen orientation on the elastic energy released.*

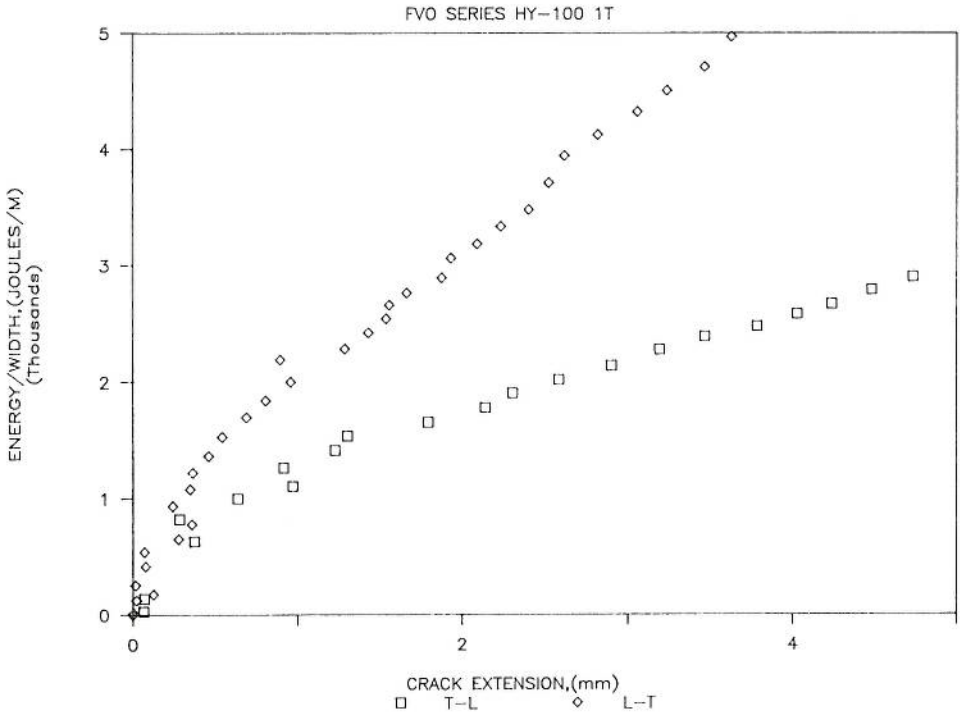

FIG. 19—*Effect of specimen orientation on the plastic energy dissipated.*

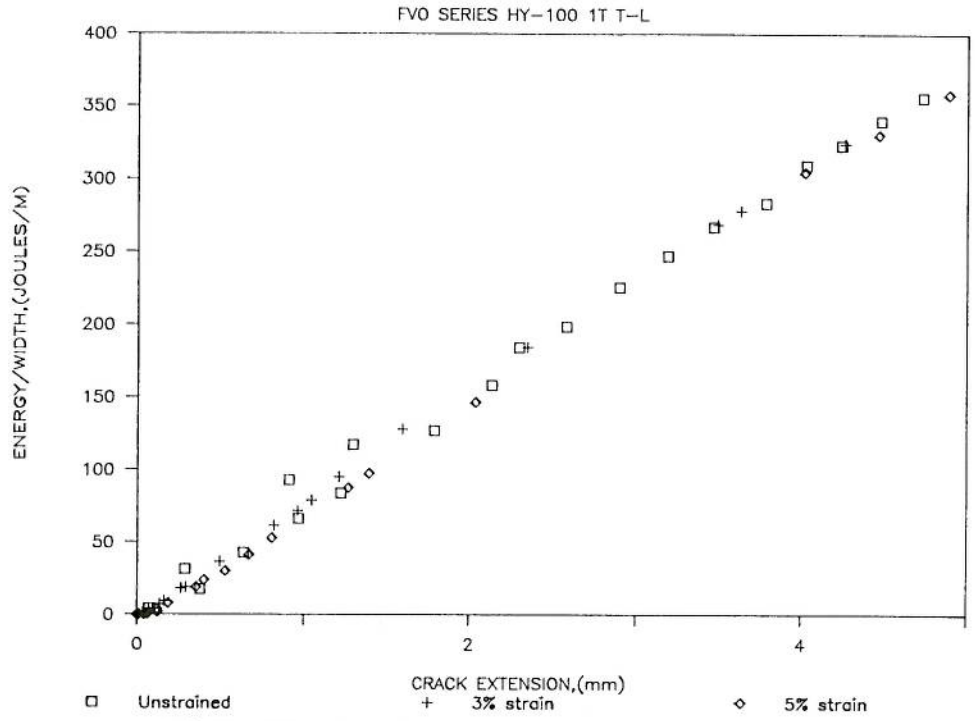

FIG. 20—*Effect of uniaxial prestraining on the elastic energy released.*

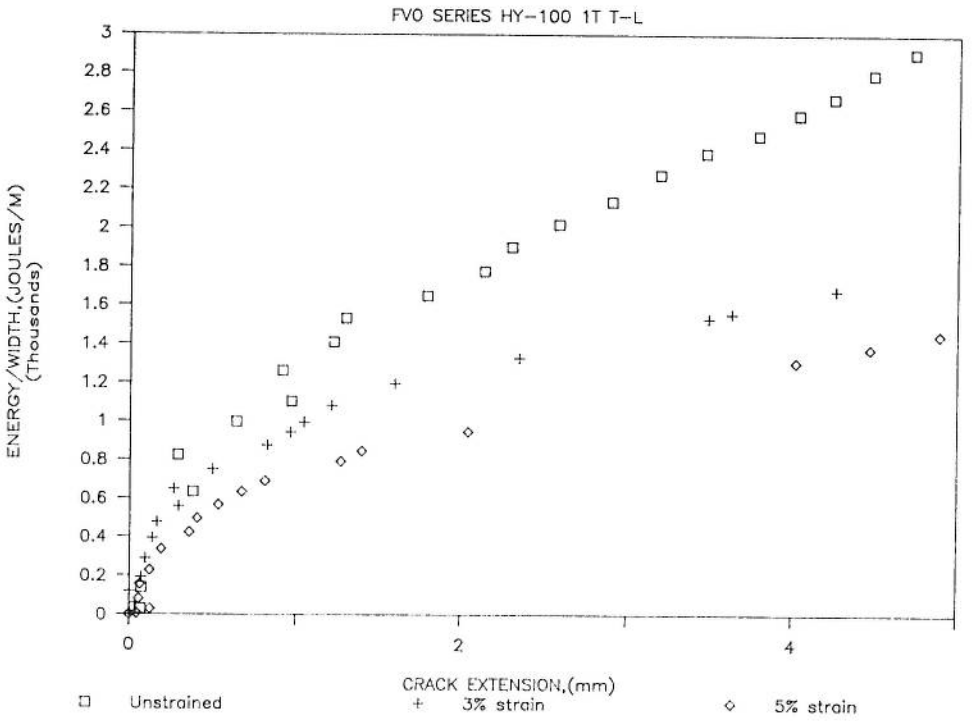

FIG. 21—*Effect of uniaxial prestraining on the plastic energy dissipated.*

The results of this evaluation for Specimen FVO1 are shown in Fig. 22. Also plotted on Fig. 22 is the *J-R* curve for this specimen evaluated using standard existing techniques [*4*]. For this latter case, J is evaluated from deformation plasticity using the definition

$$J = -\int \frac{dP}{da} d\delta = -\int \frac{d\delta}{da} dP$$

where $d\delta$ equals the increment of load-line displacement, and is taken to represent the intensity of the stress and strain singularity at the crack tip in accordance with the Hutchinson-Rice-Rosengren (HRR) singularity of Hutchison [*5*] and Rice [*6*]. The *J*-integral is also presented by Paris [*7*] as the total energy passing to the crack tip per unit of crack extension. From this point of view our experimentally measured quantity represents the energy rate flow to the specimen as a whole, and this is large while the plastic zone is developing and falls to a near constant value as steady-state crack growth conditions develop. The immediate question is, of course, which method is correct, and that depends on what question is to be answered. If one wants to determine the total released and dissipated energy associated with crack growth (that is, the total resistance to crack growth) in a body, then the energy separation method provides that solution. If one, on the other hand, wants an estimate of the energy released or dissipated in the fracture process zone only, then, perhaps, the current *J*-integral method provides this quantity. It is worth commenting, however, that it seems difficult to disassociate energy released or dissipated near the crack tip from altered energy states in the remaining part of the body, for all the forms of energy contribute to crack

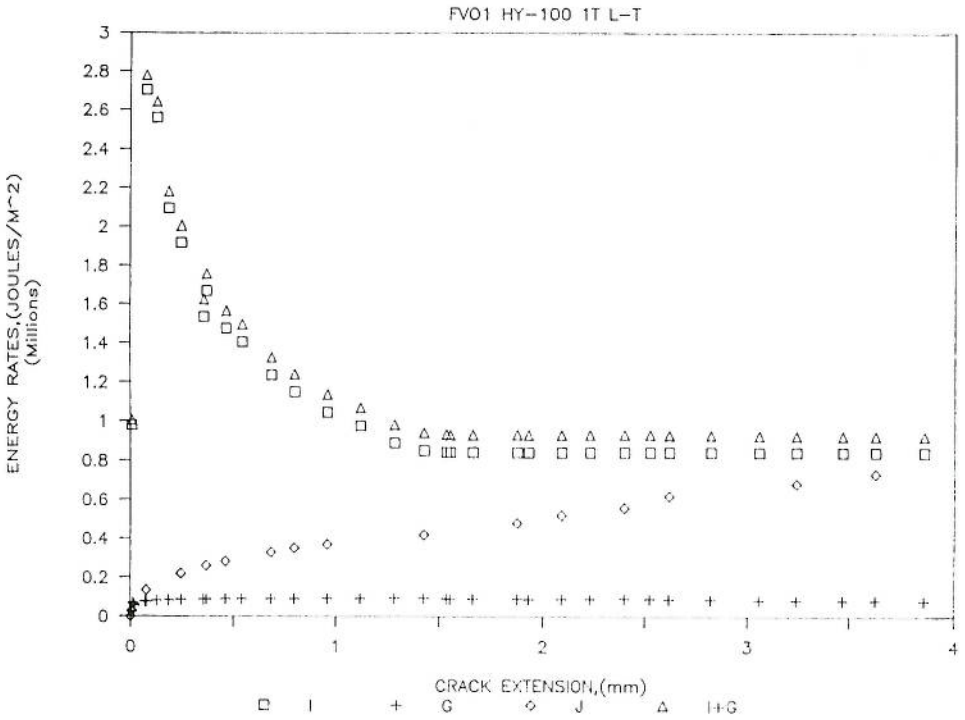

FIG. 22—*Elastic, plastic, and total energy release rates compared with the* J-R *curve obtained by the current method.*

growth resistance. If equilibrium in the body is to be maintained, the stress released at the crack tip must be balanced by alterations of stress on the compression side of the neutral axis in a bend-type CT specimen.

Conclusions

For analysis of an unloading compliance elastic-plastic fracture toughness test, the area under the load displacement record should be viewed as consisting of three rather than two components. These areas are identified here as a stored elastic energy component (which is clearly specimen dependent), an elastic energy release component, and a plastic dissipation component. These components can be separated and evaluated from standard unloading compliance data. The separation procedure was applied to several cases, and the principal conclusions are the following:

1. The elastic energy release rate measured directly from the load displacement record is nearly constant for the extent of crack extension observed.
2. The elastic energy release rate measured directly is equal to an elastic strain energy release rate, G_q, calculated from the standard elastic singularity equation for K_q from ASTM Test E 399-83, using the load value at the given location on the load-displacement record.
3. The elastic energy release rate measured directly, as defined in this study, is equal to the elastic component of the J-integral as calculated by the present ASTM recommended procedure [*4*].
4. The elastic energy release rate is dependent on both the crack size and the size of the specimen tested, at least for compact specimen analysis.
5. The plastic energy dissipation rate, I, as defined here, represents the plastic energy dissipated in the entire specimen per unit of crack extension. The value of this energy release rate is substantially higher at crack initiation than that calculated by the current J-integral procedure, but the results of both methods appear to approach each other as steady-state crack growth develops.
6. The energy quantity J is the upper bound to a J-type quantity since it represents the total energy dissipated or released during ductile crack growth.
7. While orientation of the specimen greatly affects the plastic component of energy dissipated during crack growth, it does not effect the elastic energy released.
8. Prestraining a material up to 5% prior to testing reduces the plastic energy dissipated, but leaves the elastic energy release rate unaltered.
9. Both the elastic energy release rate and the plastic energy dissipation rate, as defined here, are nearly independent of the specimen size when normalized by the uncracked remaining ligament.

References

[*1*] Vassilaros, M. G., Joyce, J. A., and Gudas, J. P., "Effects of Specimen Geometry on the J_I-R Curve for ASTM A533B Steel," *Fracture Mechanics: Twelfth Conference, ASTM STP 700,* American Society for Testing and Materials, Philadelphia, 1980, p. 251–270.

[*2*] McCabe, D. E., Landes, J. D., and Ernst, H. A., "An Evaluation of the J_R-Curve Method for Fracture Toughness Characterization," *Elastic-Plastic Fracture: Second Symposium,* Vol. II, *Fracture Curves and Engineering Applications, ASTM STP 803,* American Society for Testing and Materials, Philadelphia, 1983, pp. II-562–II-581.

[*3*] Mulligan, J. N., "Fracture Toughness Degradation in HY80 and HY100 after Prestraining," DTNSRDC

Report No. DTNSRDC-SME-CR-13-84, engineering thesis, U.S. Naval Postgraduate School, Monterey, CA, November 1984.

[4] Albrecht, P., Andrews, W. R., Gudas, J. P., Joyce, J. A., Loss, F. J., McCabe, D. E., Schmidt, D. W., and Van Der Sluys, W. A., "Tentative Test Procedure for Determining the Plane Strain J_I-R Curve," *Journal of Testing and Evaluation*, Vol. 10, No. 6, November 1982, pp. 245–251.

[5] Hutchinson, J. W., "Singular Behavior at the End of a Tensile Crack in a Hardening Material," *Journal of the Mechanics and Physics of Solids*, Vol. 16, 1968, pp. 13–31.

[6] Rice, J. R. and Rosengren, G. F., "Plane Strain Deformation Near Crack Tip in a Power Law Hardening Material," *Journal of the Mechanics and Physics of Solids*, Vol. 16, 1968, pp. 1–12.

[7] Paris, P. C., "Fracture Mechanics in the Elastic-Plastic Regime," *Flow Growth and Fracture: Tenth Conference, ASTM STP 631*, Philadelphia, 1977, pp. 3–27.